HILO2K: A COUPLED NEUTRON-PHOTON TRANSPORT CROSS-SECTION LIBRARY FOR NEUTRON ENERGIES UP TO 2000 MEV

R. A. Lillie and F. X. Gallmeier
Oak Ridge National Laboratory
P. O. Box 2008
Oak Ridge, TN 37831-6363
(423) 574-6083

ABSTRACT

HILO2k is a new high-energy neutron and photon transport cross-section library containing neutron cross sections to 2 GeV and photon cross sections to 20 MeV. This library is the culmination of work directed at producing a high-energy multigroup transport library suitable for use in multidimensional deterministic transport codes. Its development was funded by neutronics R&D funds from the planned Spallation Neutron Source (SNS) project. It is also a modified extension of the preliminary HILO library (HILO1k) presented at the AccApp'99 meeting.

I. INTRODUCTION

The new HILO2k library contains ANISN[1] formatted cross sections for neutron energies up to 2 GeV and photon energies up to 20 MeV for 32 nuclides. The upper neutron energy of 2 GeV was chosen because it is possible that the SNS may go to approximately 1.4 GeV, and proposed accelerator facilities with proton energies between 1 and 2 GeV are currently being studied for other than neutron scattering purposes. The high-energy neutron cross sections (E > 20 MeV) in HILO2k are based on high-energy doubly differential neutron interaction data and neutron and photon production data generated with a modified version of MCNPX.[2, 3] The low-energy (E < 20 MeV) cross sections for both neutrons and photons are based on ENDF data. In addition to transport cross sections, the new HILO library contains flux-to-dose conversion factors and kermas (nuclear heating response functions) for all energies for all 32 nuclides. It also contains dpa and ^{1}H and He gas production response functions covering selected energy ranges for some of the nuclides comprising structural materials.

There are several significant differences between HILO2k and the preliminary HILO library[4] (HILO1k) presented at the AccApp'99 meeting besides the change in upper neutron energy from 1 to 2 GeV. The major difference in the two libraries is that all of the high-energy neutron interaction and neutron and photon production data used to build HILO2k was obtained from MCNPX employing the Bertini intra-nuclear cascade model (INC model)[5]. In building HILO1k, this data was generated employing both the INC model and the Cascade-Exiton Model (CEM97)[6]. (A detailed discussion of why both nuclear models were employed is presented in Ref. 4 and will not be reproduced here). The decision to use only the INC model was predicated by the appearance of numerical instabilities in the coupling between CEM97 and the PHT photon production model[7] for the highest incident neutron energies. These instabilities appeared when treating only 12 nuclides, i.e., Na through Cu. However, when these instabilities were eliminated, other numerical difficulties arose. In addition, larger nonelastic interaction cross sections were obtained using the INC model and these cross sections were in somewhat better agreement with available experimental data, particularly in the 150 to 400 MeV energy range.

II. DATA GENERATION AND ANALYSIS

All of the MCNPX calculations performed to obtain particle interaction and production data used a finite radius spherical model to allow particle transport. Particle transport was allowed to approximately account for the secondary neutrons produced by the charged particles exiting both primary (initial neutron interaction) and secondary collisions (charged particle interactions only). Normally, secondary neutrons produced by secondary charged particles are not treated when generating data for transport cross sections. However, as incident neutron energy increases, the number of secondary neutrons produced some distance from the initial interaction site also increases. If cross-section data were being generated for an element (versus an isotope of an element, e.g., ^{10}B), the sphere consisted of all isotopes comprising more than 1 weight percent of that element. The theoretical density of all elements was used except for gaseous elements in which case an arbitrary density of 0.1 g/cc was employed.

Modifications were made to MCNPX to output neutron production, photon production, and charged

particle kinetic energy data. The charged particle kinetic energy data was needed to generate high-energy neutron kerma factors for HILO2k. In addition, a number of modifications were made for accounting purposes since particle transport was allowed. First, all primary collisions were forced to occur at the center of the 0.5 m radius sphere. This allowed all secondary collisions to be identified by simply outputting the position of each collision. Second, once the necessary data for all neutrons exiting either a primary or secondary collision was obtained, these neutrons were "killed" so that they could not produce additional neutrons. Neutrons produced by neutrons exiting collisions were accounted for in separate lower-energy incident neutron calculations.

The number of incident neutrons chosen for each nuclide at each incident energy in the MCNPX data production runs was determined using a simple bin-varying algorithm. This algorithm predicted energy group (bin) boundaries such that each energy bin essentially contained an equal number of secondary neutrons and thus had almost equal Monte Carlo uncertainties. Equal uncertainties allowed an accurate estimate to be made of the number of incident neutrons required for acceptable uncertainties. In this work, an uncertainty of 1% on each energy bin was assumed to be small enough to ensure that variations in the produced data were not due to Monte Carlo statistics. The algorithm was based on the assumption that the number of produced neutrons in any energy bin was proportional to the width of that bin.

Multigroup transport libraries for deterministic transport codes generally contain Legendre coefficients to represent the angular dependence of scattering. The energy dependent Legendre coefficients in HILO2k were obtained directly from the individual particle data generated by MCNPX. They were not obtained by summing (integrating) angular binned data. Each exiting neutron (or photon) was assumed to come from a single discrete scattering event. Thus, the contribution of each exiting neutron to the n^{th} scattering Legendre coefficient was obtained by simply evaluating the n^{th} Legendre polynomial at the cosine of the angle between the incident neutron direction and the exiting neutron direction.

The nonelastic scattering Legendre coefficients were obtained by summing over all neutrons exiting nonelastic collisions and multiplying by the geometric cross section divided by the number of incident neutrons. The elastic scattering Legendre coefficients were obtained by summing over all neutrons exiting elastic collisions and multiplying by the elastic scattering cross section divided by the number of elastic collisions. Adding both sets of coefficients together produced the properly normalized within-group and group-to-group energy dependent Legendre coefficients. Determining the coefficients in this manner made use of the maximum amount of angular information in generating each coefficient. However, actual angular dependent scattering distributions are not obtained. (For compatibility with Oak Ridge transport codes, each n^{th} order Legendre coefficient was multiplied by 2n+1).

The nonelastic interaction cross sections in HILO2k were obtained by multiplying the geometric cross section by the number of nonelastic collisions (number of attempted nonelastic collisions minus the number of pseudo collisions) and dividing by the number of attempted nonelasitc collisions. The elastic interaction cross sections in HILO2k were obtained directly from the elastic scattering cross sections output by MCNPX. Summing these two interaction cross sections produced the total cross sections in HILO2k.

III. HILO2k LIBRARY DESCRIPTION

A. List of Nuclides

The 32 nuclides in the HILO2k library are listed in Table I. For all of the nuclides except Zr, Cd, Gd, and Hg, the low-energy neutron and photon cross sections were obtained by collapsing the ENDF/B-VI based VITAMIN-B6 fine group library.[8] The low-energy cross sections for these nuclides were obtained by collapsing the ENDF/B-V based VITAMIN-E fine-group library[9] since photon production data for these elements was not present in the VITAMIN-B6 library. The low-energy cross sections for Hg were obtained by processing Howerton data[10]. In addition, the high-energy ($19.64 < E < 150$ MeV) nonelastic interaction and production data for ^{2}H, C, N, O, Al, Si, Ca, Cr, Fe, Ni, Cu, Nb, W, and Pb, were normalized to the nonelastic interaction cross sections contained in the LANL 150 MeV cross-section library[11].

Table I. List of Nuclides in HILO2k Library

^{1}H	^{2}H	He	Be	^{10}B	^{11}B	C	N
O	Na	Mg	Al	Si	S	K	Ca
Cr	Mn	Fe	Ni	Cu	Zr	Nb	Cd
Ba	Gd	Ta	W	Hg	Pb	^{235}U	^{238}U

The high-energy neutron kermas in HILO2k were obtained from charged particle production data generated with MCNPX. The low-energy neutron kermas were obtained from the KAOS library[12] for all nuclides except Cd, Ba, Gd, and Hg. For Cd, Ba, and Hg, the kermas were obtained from LENDL data[13] whereas the Gd

kermas were obtained from the LANL(T-2) kerma data contained in the MCNPX low energy cross-section library. The photon kermas were obtained from the Vitamin-B6 library for all nuclides except Zr, Cd, Ba, Gd, and Hg. The Hg photon kermas were obtained from the Howerton data.[10] Kermas for Zr, Cd, Ba, and Gd were obtained from the Vitamin-E library. The flux-to-dose conversion factors were obtained from the Georgia Institute of Technology[14] and the dpa and gas production cross sections were obtained from North Carolina State University.[15]

B. Energy Group Structure

The energy group structure of the new HILO2k library is given in Tables II-a,b, and c. The high-energy (E > 19.64 MeV) neutron group boundaries are given in Table II-a. These energies also represent the incident neutron energies employed in the MCNPX calculations. The low energy neutron (E < 19.64 MeV) and photon (E < 20 MeV) group boundaries are given in Tables II-b and II-c, respectively.

Table II-a. HILO2k High Energy (E > 19.64 MeV) Neutron Group boundaries

Grp No.	Upper Energy (MeV)	Grp No.	Upper Energy (MeV)	Grp No.	Upper Energy (MeV)
1	2000.0	15	700.0	29	200.0
2	1850.0	16	650.0	30	180.0
3	1700.0	17	600.0	31	160.0
4	1550.0	18	550.0	32	150.0[a]
5	1400.0	19	500.0	33	140.0
6	1300.0	20	450.0	34	120.0
7	1200.0	21	400.0	35	100.0
8	1100.0	22	375.0	36	80.0
9	1000.0	23	350.0	37	70.0
10	950.0	24	325.0	38	60.0
11	900.0	25	300.0	39	50.0
12	850.0	26	275.0	40	40.0
13	800.0	27	250.0	41	30.0
14	750.0	28	225.0	42	25.0

[a] This boundary was chosen to facilitate coupling to LANL 150 MeV Library.

Both low-energy group structures have been changed from those employed in the preliminary HILO1k library and the original HILO library.[16] The number of low energy neutron groups has been increased from 37 to 41. This increase was primarily made to provide greater energy resolution at the 22 keV Fe window. Increasing the energy resolution was particularly important for the SNS since a large amount of low carbon steel is present in the current target monolith design. The number of photon groups was kept at 22. However, the photon energy group structure was changed to facilitate transport of activation photons.

Table II-b. HILO2k Low Energy (E < 19.64 MeV) Neutron Group boundaries

Grp No.	Upper Energy (MeV)	Grp No.	Upper Energy (MeV)	Grp No.	Upper Energy (MeV)
43	19.64	57	2.232	71	2.418-2
44	16.91	58	1.827	72	2.188-2
45	14.92	59	1.423	73	1.503-2
46	14.92	60	1.108	74	3.355-3
47	12.21	61	8.209-1[a]	75	1.585-3
48	10.0	62	7.427-1	76	4.540-4
49	8.607	63	6.081-1	77	2.145-4
50	7.408	64	4.979-1	78	1.013-4
51	6.065	65	3.688-1	79	3.727-5
52	4.966	66	2.472-1	80	1.068-5
53	3.679	67	1.575-1	81	3.059-6
54	3.012	68	1.111-1	82	1.125-6
55	2.466	69	5.248-2	83	4.140-7
56	2.346	70	3.183-2		1.0-11[b]

[a] 8.209-1 read as 8.209×10^{-1}.
[b] 1.0-11 is the lower energy of last neutron group 83.

Table II-c. HILO2k Photon Group boundaries

Grp No.	Upper Energy (MeV)	Grp No.	Upper Energy (MeV)	Grp No.	Upper Energy (MeV)
84	20.0	92	4.0	100	6.0-1
85	14.0	93	3.0	101	4.5-1
86	12.0	94	2.5	102	3.0-1
87	10.0	95	2.0	103	1.5-1
88	8.0	96	1.5	104	7.0-2
89	7.0	97	1.0	105	4.5-2
90	6.0	98	8.0-1[a]		1.0-2[b]
91	5.0	99	7.0-1		

[a] 8.0-1 read as 8.0×10^{-1}.
[b] 1.0-2 is the lower energy of last photon group 105.

C. Current Library Versions

Four versions of the new HILO library have been constructed. Standard and modified versions have been constructed both with and without the nonelastic

interaction and production data normalized to the LA-150 library nonelastic interaction cross sections. In the standard version, all high-energy particle interaction and production data was taken into account to obtain the group total cross section (interaction cross section) and the group-to-group Legendre coefficients (scattering cross sections). In the modified version, not all of the neutrons were taken into account. In this version, rejection criteria were applied to neutrons exiting both elastic and nonelastic collisions with all nuclides except ^{1}H. (^{1}H was treated the same in both libraries). Neutrons exiting a collision with scattering angle cosines greater than 0.99 and having more than 95 % of the incident neutron energy were ignored in determining the Legendre coefficients and the collisions producing these neutrons were also ignored. Ignoring these neutrons results in reduced scattering cross sections. Ignoring these collisions results in reduced interaction cross sections. Reducing the scattering and interaction cross sections in this manner is equivalent to assuming that these neutrons may be accurately represented as uncollided particles. In the earlier HILO1k library[4] slightly different rejection criteria were applied to only elastic collisions and then only for nuclides having atomic numbers smaller than 73. For the remaining nuclides, all elastic scattering was ignored.

The rejection criteria were changed and extended to treat nonelastic scattering because difficulties were encountered in a number of multi-dimensional (two-dimensional R-Z cylindrical and three-dimensional X-Y-Z rectangular) discrete ordinates calculations performed in the ongoing SNS shielding analysis. These difficulties surfaced during rebalance acceleration and were primarily due to the generation of negative scattering sources. The negative scattering sources resulted from the use of low order P_5 Legendre expansions to represent the angular dependence of the scattering cross sections. P_5 expansions can not adequately represent the straight ahead or highly forward peaked portion of the nonelastic produced neutrons at high incident neutron energies. The use of higher order expansions was not possible because of extremely large computer storage requirements. All four versions of the new HILO2k library contain P_9 Legendre expansions for the scattering cross sections.

D. Library Structure

Both standard and modified libraries have been generated in compressed ascii form for portability to other platforms and an interactive fortran code entitled LCMT (Library Conversion, Modification, & Truncation) has been written to convert these compressed ascii libraries to binary ANISN formatted libraries. This code may also be used to perform P_n corrections and to create smaller truncated versions of both libraries. In LCMT, P_n corrections indicate that the within group or self-scatter P_n coefficients are replaced with modified coefficients plus dirac-delta functions to approximate almost straight ahead scattering. In the resulting P_N expansion, the P_N within group coefficients become zero and the lower order coefficients are reduced by the P_N coefficient. The dirac-delta functions are accounted for by also reducing the group total interaction cross sections. The truncated versions output by LCMT are constructed by removing higher order P_n components and by removing the highest energy groups, e.g., a P_5 library having an upper neutron energy of 1 GeV could be constructed. In all cases, a file listing of the title records contained in the output ANISN binary library is written and the reduced output library table length is appropriately adjusted.

All four versions of the new HILO2k library contain 105 total energy groups (42 high-energy neutron, 41 low-energy neutron, and 22 photon groups as listed in Table II). The total cross_section for each group is located in table position 9 and the within group self-scatter cross section is located in table position 10 resulting in a table length of 114. For neutron energies below 19.64 MeV and photon energies below 20 MeV, the absorption cross section for each group is located in position 7 and where applicable, the number of fission neutrons times the fission cross section is located in position 8. Both versions contain 5 activity materials with materials ID's 1000 through 5000. Material 1000 contains total, neutron, photon, neutron (E > 19.64 MeV), and neutron (E < 19.64 MeV) flux-to-dose conversion factors, dpa and gas production cross sections, and several flux energy integrating functions. Materials with ID's 2000 through 5000 contain total, neutron, photon, neutron (E > 19.64 MeV), and neutron (E < 19.64 MeV) kermas with units of watts/gram per unit flux. In addition, the P_0 component of each material contains these same kerma response functions in table positions 1 through 5 with units of (Joule-barns)/atom to allow the straightforward generation of mixed material kermas, e.g., concrete, water, stainless steel, etc.

IV. INITIAL TEST RESULTS

A number of one-dimensional spherical calculations have been performed to test the new HILO2k library. Particle leakage calculations employing the new HILO2k library were carried out using the one-dimensional discrete ordinates code ANISN. Leakage spectra from one-meter radius spheres made of lead, 1020 steel, and ordinary concrete have been separately calculated and compared against leakages calculated with MCNPX. These materials were chosen for the initial test calculations since 1020 steel and ordinary concrete are

two of the primary materials being used for much of the SNS shielding. In addition, lead was strongly considered as a possible candidate for the SNS target monolith shielding because of cost considerations.

Neutron leakage spectra from a one-meter radius 1020 steel sphere are presented in Fig. 1 for a 975 MeV isotropic neutron source located at the center of the sphere. The MCNPX calculation was performed using a neutron lower energy cutoff of 150 MeV, i.e., the Bertini Intranuclear Cascade was only employed for neutron energies above 150 MeV. Below 150 MeV, all neutron interactions were treated using the LA-150 cross-section data. In addition, the uncertainties associated with each energy bin are between 1 and 3 %. For consistency, the modified version of HILO2k employed in the ANISN calculation contained nonelastic cross sections normalized to the LA-150 data. In addition, all of the ANISN calculations were carried out using P_5 Legendre expansions since P_5 is very likely the maximum usable order of scattering in most multidimensional transport calculations.

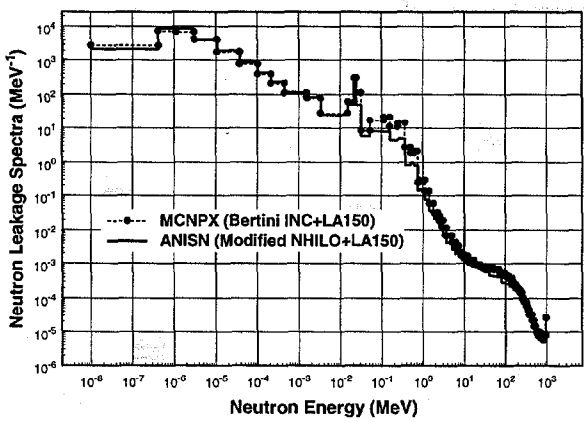

Fig.1. Neutron Leakage Spectra from a 1 m radius 1020 Steel Sphere due to a 975 MeV Isotropic Neutron Source at the Center of Sphere

The overall agreement between the two leakage spectra in Fig. 1 is very good except in the 40 to 500 keV range where the leakage calculated with ANISN (HILO2k) appears low. Similar agreement was obtained when the calculations were performed without employing the LA-150 data. One interesting point to note is the sharp peak in both spectra at the 22 keV Fe window. This is a direct result of the better energy resolution in HILO2k at the Fe window.

In Fig. 2, these same leakage spectra are again presented for neutron energies above 10 MeV to provide more resolution in the high-energy range. In addition, the spectrum obtained using the standard library (normalized to the LA-150 data) is also presented. With the better resolution, it becomes apparent that calculations performed with both libraries underestimate the neutron leakage considerably between 40 and 150 MeV and coincidentally this is the energy range where both libraries have been normalized to the LA-150 data. However, the normalization has nothing to do with the underestimates as similar underestimates over the same energy range are obtained when the LA-150 data is not used. However, of more interest is the factor of 10 underestimate in the source group leakage, i.e., between 0.95 and 1.0 GeV, when the standard HILO2k library is employed in ANISN. This underestimate results from the low order P_5 Legendre expansion's inability to represent the highly forward peaked elastic scattering. Instead of allowing source particles to forward scatter with little if any energy loss, these particles downscatter as evidenced by the overestimate of the leakage between 700 and 950 MeV. These effects are not seen when the modified HILO2k library is employed since the highly forward scattered particles are represented by uncollided particles.

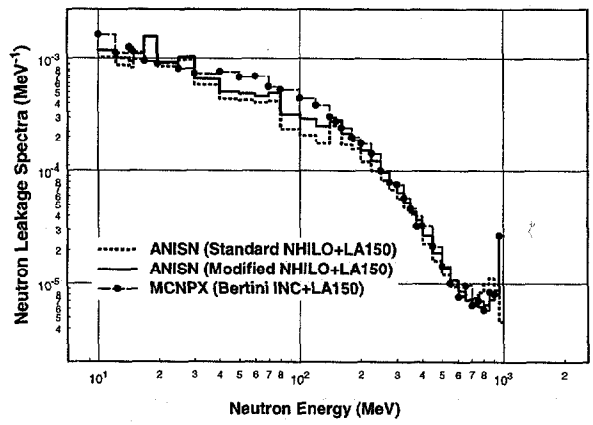

Fig.2. Neutron Leakage Spectra from a 1 m radius 1020 Steel Sphere (10 – 1000 MeV only)

To better illustrate the effect of ignoring forward scattered particles in building the modified versions of the new HILO2k libraries, the neutron leakage spectra from a one-meter radius lead sphere are presented in Fig. 3 over the energy range from 10 to 1000 MeV. As in the 1020 steel calculations, these spectra were obtained for a 975 MeV isotropic neutron source located at the center of the lead sphere. The LA-150 data was not employed in these calculations. The Bertini INC model was employed in MCNPX for all neutron interactions above 19.64 MeV. The number of source neutrons in the

MCNPX calculation was again chosen to obtain 1 to 3 % uncertainties on all energy bins and P_5 scattering was again employed in both ANISN calculations.

The agreement between the ANISN and MCNPX results for the lead sphere is generally much better than that obtained for the 1020 steel sphere. The considerable underestimate of the leakage in the intermediate energy range only occurs between 80 and 120 MeV and it only occurs when using the standard HILO2k library. However, the factor of 10 underestimate of the leakage between 950 and 1000 MeV and the overestimate of the leakage between 700 and 950 MeV are again present when using the standard library.

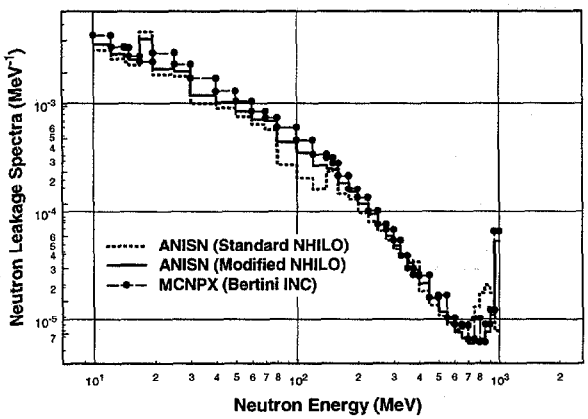

Fig.3. Neutron Leakage Spectra from a 1 m radius Lead Sphere due to a 975 MeV Isotropic Neutron Source at the Center of Sphere

The effect on the energy dependent total interaction cross section for lead when the particle rejection criteria are used to build the modified HILO2k libraries is illustrated in Fig. 4. As stated above, the rejection criteria discards neutrons exiting a collision with a scattering angle cosine greater than 0.99 and an energy greater than 95 % of the incident neutron energy. These neutrons are thus ignored in the generation of the doubly differential scattering cross sections (energy dependent Legendre scattering coefficients) and the total interaction cross sections.

Between 60 and 120 MeV the total interaction cross section for lead is reduced by almost a factor of two. This factor of two reduction is most likely the reason the modified library produces much better agreement in the neutron leakage spectra from the lead sphere between 60 and 120 MeV. Above 200 MeV, the reduction increases from approximately 30 % to slightly more than 40 % between 1 and 2 GeV. The reduction at 1 GeV is obviously responsible for the excellent agreement of the within group leakage, i.e., the leakage between 950 and 1000 MeV.

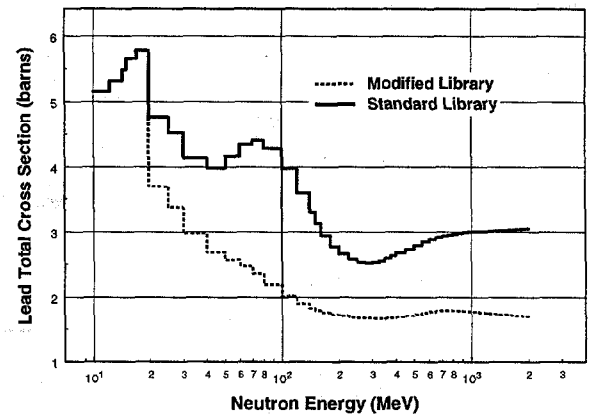

Fig.4. Comparison of Lead Total Cross Section in Standard and Modified New HILO2k Libraries

The percent reductions in both the elastic and nonelastic components of the lead total interaction cross section are presented in Fig. 5.

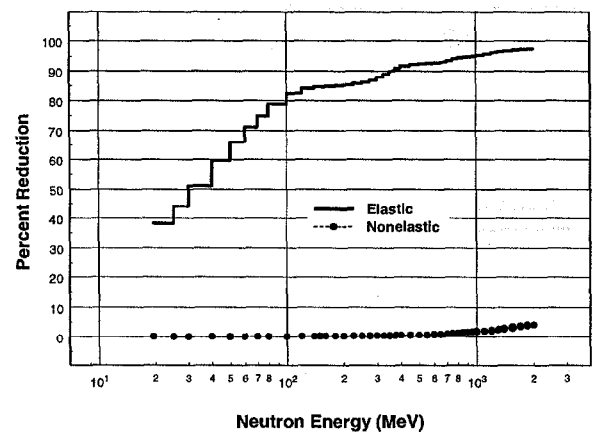

Fig.5. Percent Reduction in Lead Elastic and Nonelastic Cross Sections in Modified New HILO2k Libraries

It is obvious from Fig. 5 that the primary reduction in the total cross section is due to the large reduction in the elastic scattering cross section. At 1 GeV, the application of the rejection criteria results in a 97 % reduction in the elastic scattering cross section and only a

3 % reduction in the nonelastic scattering cross section. Thus as expected it is the elastic cross section that dominates the highly forward peaked scattering. In fact, as illustrated in Fig. 6, better agreement in the neutron leakage spectra from the lead sphere results when elastic scattering is totally ignored when generating the lead cross sections.

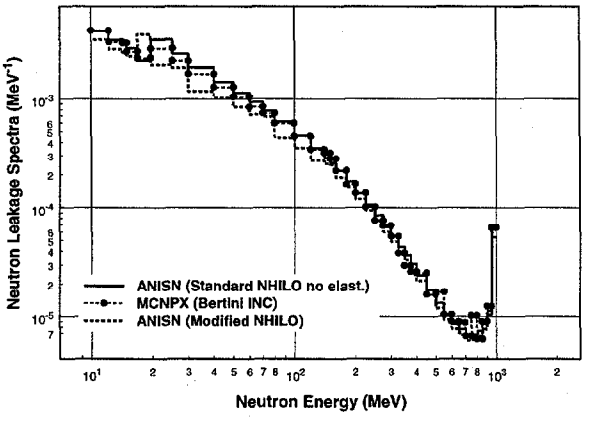

Fig.6. Neutron Leakage Spectra from a 1 m radius Lead Sphere due to a 975 MeV Isotropic Neutron Source at the Center of Sphere

Excellent agreement is obtained in the neutron leakage spectra from the lead sphere when elastic scattering is ignored especially at neutron energies above 40 MeV. Below 40 MeV, the absence of elastic scattering results in overestimates of the leakage. However these overestimates are much smaller than the underestimates over this energy range and extending to approximately 120 MeV when even the reduced elastic scattering cross sections are employed. In addition, the overestimates are conservative from a shielding point of view.

A comparison of the neutron leakage spectra above 10 MeV from a one-meter radius concrete sphere is presented in Fig. 7. As in the lead calculations, the MCNPX calculation and both ANISN calculations were performed without using the LA-150 cross section data. The results are similar to those obtained for the 1020 steel using the LA-150 data since the ANISN calculations produce considerable underestimation of the neutron leakage in the 30 to 140 MeV energy range. However, at the higher neutron energies, i.e., above 700 MeV, the leakages obtained with the standard library agree almost as well as those obtained with the modified library.

In view of these comparisons, it is readily apparent that P_5 Legendre coefficients cannot adequately represent the high degree of scattering anisotropy present at high neutron energies particularly in high energy elastic collisions. The obvious solution to this dilemma is to simply employ higher order Legendre expansions to represent the angular dependence of neutron elastic scattering and/or nonelastic production. As noted above, this is not possible in most multidimensional transport calculations because of computer storage limitations. However, even if this were not the case, some very preliminary results from additional one dimensional calculations performed for lead using much higher Legendre expansions, e.g., P_{39} to P_{199}, indicate that high-order expansions are not adequate at high energies especially for elastic scattering. The solution, at least for lead, appears to be to simply ignore elastic scattering.

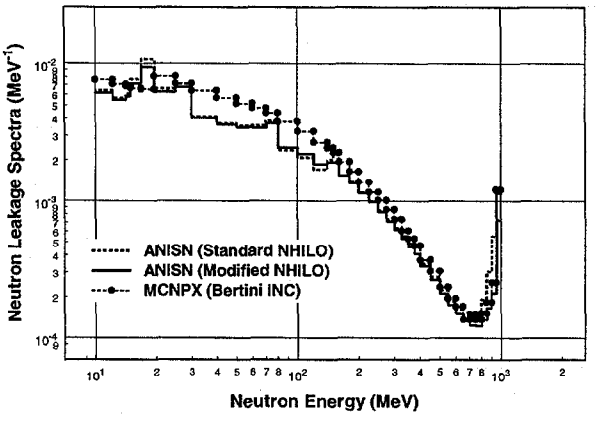

Fig.7. Neutron Leakage Spectra from a 1 m radius Concrete Sphere due to a 975 MeV Isotropic Neutron Source at the Center of Sphere

Additional calculations are being performed to further test the new HILO2k libraries. In these calculations, spatially dependent flux spectra, outward directed leakage spectra, and personnel dose will be compared for lead, ordinary and heavy concrete, 1020 steel, earth, and several other materials as a function of gram thickness up to a maximum gram thickness of 2000 grams. Since kerma factors were also generated in the present effort, volume averaged nuclear heating or energy deposition rates will also be compared. These comparisons will be performed for a number of incident neutron energies. To perform the MCNPX calculations, weight windows based on adjoint fluxes from ANISN will be employed. It is hoped that the results from these calculations will lead to a better representation of straight ahead scattering and result in a single version of the new HILO2k library (normalized to the LA-150 nonelastic

data). In addition, beta test releases of all four versions together with the LCMT code are also being prepared.

V. SUMMARY

A new multigroup transport cross-section library (HILO2k) containing high-energy neutron interaction and production cross sections and response functions has been generated for 32 nuclides. The total number of energy groups in HILO2k is 105, i.e., 42 high-energy neutron groups, (19.64 MeV < E < 2 GeV), 41 low-energy neutron groups, (10^{-5} eV < E < 19.64 MeV), and 22 photon groups, (10 keV MeV < E < 20 MeV). All high-energy neutron interaction and production data was obtained from MCNPX calculations employing the Bertini Intranuclear Cascade model. For testing purposes, standard and modified versions of the new HILO2k library have been constructed. In the standard versions, all high-energy neutron interaction and production data was taken into account whereas in the modified versions, some of this data was ignored in an attempt to better approximate straight ahead scattering. Results form initial transport test calculations indicate that the modified versions generally produce better agreement with results obtained using MCNPX. Testing of the library is ongoing and beta test releases are in final preparation.

REFERENCES

1. W. W. Engle, Jr., "ANISN, A One Dimensional Discrete Ordinates Transport Code with Anisotropic Scattering", Oak Ridge Gaseous Diffusion Plant, K-1693 (1967). (See also RSICC Computer Code Center Collection Document CCC-82)

2. H. G. Hughs, R. E. Prael, and R. C. Little, "MCNPX-The LAHET/MCNP Code Merger," Los Alamos National Laboratory, Tech. Rept. XTM-RN(U) 96-012 (1997).

3. Franz X. Gallmeier, "Implementation of the CEM-Code into the MCNPX-Code," *Proc. of the Fourth Workshop on Simulating Accelerator Radiation Environments, Knoxville*, TN, Sept. 14-16, 1998, p131, Oak Ridge National Laboratory (1998).

4. R. A. Lillie and F. X. Gallmeier, "HILO Transport Cross-Section Library Extension," *Proceedings of the Third International Topical Meeting on Nuclear Applications of Accelerator Technology*, Long Beach, CA (1999).

5. H. W. Bertini, *Phys. Rev.* 188, 1711 (1969).

6. S. G. Mashnik, A. J. Sierk, O. Bersillon, and T. A. Gabriel, "Cascade-Exiton Model Detailed Analysis of Proton Spallation at Energies for 10 MeV to 5 GeV," *Nucl. Instr. Meth* A414, 68 (1998).

7. R. E. Prael and H. Lichtenstein, "Users Guide to LCS: The LAHET Code System," Los Alamos National Laboratory, LA-UR-89-3014 (1989).

8. J. E. White, et. al., "VITAMIN-B6: A Fine-Group Cross Section Library Based on ENDF/B-VI for Radiation Transport Applications," *Proceedings of the International Conference on Nuclear Data for Science and Technology*, Gatlinburg, TN (1994).

9. R. W. Roussin, et al., "VITAMIN-E: A Coupled 174-Neutron, 38-Gamma-Ray Multigroup Cross-Section Library for Deriving Application-Dependent Working Libraries for Radiation Transport Calculations," Oak Ridge National Laboratory, ORNL/RSIC Report (1987).

10. R. J. Howerton, Lawrence Livermore National Laboratory, private communication (data in RSICC).

11. M. B. Chadwick, et. al., "LA150 Documentation of Cross Sections, Heating, and Damage," Los Alamos National Laboratory, LA-UR-99-1222 (1999).

12. Y. Farawila, U. Gohar, and C. Maynard, "KAOS/LIB-V: A library of Nuclear Response Functions Generated by KAOS-V Code from ENDF/B-V and Other Data Files," Argonne National Laboratory, ANL/FPP/TM-241 (1989).

13. R. J. Howerton and M. H. MacGregor, "The LLL Evaluated Nuclear Data Library (ENDL): Description of Individual Evaluations for Z=0-98," Lawrence Livermore National Laboratory, Livermore, California, UCRL-50400 Vol. 15 (1978).

14. N. E. Hertel, M. R. Sutton, and J. E. Sweezy, Neely Nuclear Research Center, Georgia Institute of Technology, private communication (1999).

15. M. S. Wechsler and M. H. Barnett, Department of Nuclear Engineering, North Carolina State University, private communication (1999).

16. R. G. Alsmiller, Jr., J. M. Barnes, and J. D. Drischler, "Neutron Photon Multigroup Cross Sections for Neutron Energies Less Than or Equal to 400 MeV (Revision 1)," Oak Ridge National Laboratory, ORNL/TM-9801 (1986).